Available online at www.sciencedirect.com
SCIENCE DIRECT®
Journal of Organometallic Chemistry 690 (2005) 197–210
Journal of Organometallic Chemistry
www.elsevier.com/locate/jorganchem

Imino- and bis-imino-pyridines with *N-ter*-butyl-*N*-aminoxyl group: synthesis, oxidation and use as ligand towards M^{2+} (Mn, Ni, Zn) and Gd^{3+}

Carsten Uerpmann, Bernard J.L. Henner *, Christian Guérin, Françis Carré

UMR 5637-Chimie Moléculaire et Organisation du Solide, CC 007 Université de Montpellier II, Place E. Bataillon, F-34095 Montpellier Cedex 5, France

Received 1 July 2004; accepted 10 September 2004
Available online 30 November 2004

Abstract

Imino- and bis-iminopyridine ligands bearing *N-ter*-butylhydroxy groups were synthesized by the condensation reaction between a *N-ter*-butylhydroxy substituted aniline and 2-formylpyridine, 2-acetylpyridine and 2,6-bis-acetylpyridine. The *N-ter*-butylaminoxy radicals obtained after oxidation using PbO_2 or Ag_2O were studied by EPR spectroscopy in solution. Indeed, complete decomposition was observed during isolation of these radical derivatives. The *N-ter*-butylhydroxy substituted ligands obtained were complexed with Mn^{2+}, Ni^{2+}, Zn^{2+} and Gd^{3+} salts; the obtained complexes were characterized and oxidized to give the aminoxy analogs, which were studied using IR, UV and EPR spectroscopies.

Keywords: Iminopyridines; Metal(II) complexes; Radical

1. Introduction

Much attention has been devoted since several years to the use of nitroxide free radicals as spin carriers in the design of molecular magnetic materials [1–14]. In particular, research have been done in their coordination chemistry and in the magnetic properties of their metal complexes [15–31]. This subject has been the topic of several books [32–36].

One possible way of obtaining these materials is the organic–inorganic hybrid route with one or more radicals in the organic part. This route was explored by Drillon and coworkers [37] in the case of lamellar compounds with imino-nitroxide substituted benzoate, in *para* and *meta* position; we also have obtained phenyl substituted *ter*-butylnitroxide phosphonate and -sulfonate of manganese (II), as lamellar derivatives with an inter-lamellar distance of 22 Å [38].

We wanted to extend this work to transition metal ligands bearing *ter*-butylaminoxyl groups and choose the imino- and bis-iminopyridine family of compounds. In this case, this will allow first, the formation of paramagnetic transition metal complexes bearing organic radicals and second, open the field of more extended structures with the possible complexation of the nitroxide group with another transition metal. Indeed, the donor properties of the nitroxide are poor, but coordination of this group occurs with crowded metal centres carrying electron-withdrawing groups such as, for instance, $Mn(hfac)_2$ (hfac: hexafluoroacetylacetonate).

Iminopyridine ligands are known to coordinate easily to transition metals [39–41]. in the case of bis-iminopyridines, for instance, various complexes were prepared by Brookhart et al, characterized by X-ray diffraction

* Corresponding author. Tel.: +33 467 143864; fax: +33 467 143852.
E-mail address: bhenner@univ-montp2.fr (B.J.L. Henner).

0022-328X/$ - see front matter © 2004 Elsevier B.V. All rights reserved.
doi:10.1016/j.jorganchem.2004.09.014

spectroscopy, and used as efficient catalyst for the polymerisation of ethylene and propylene [42–44].

In this paper, we describe the synthesis of iminopyridines and bis-iminopyridines with *ter*-butylaminoxyl groups. These compounds were obtained by the synthesis of *ter*-butylaminoxylanilines followed by their condensation reaction with pyridine substituted aldehydes or ketones. The as-prepared ligands were reacted with MX_n derivatives ($M^{2+} = Ni^{2+}$, Mn^{2+}; X = Cl; $n = 2$. $M^{3+} = Gd^{3+}$; $X = NO_3$; $n = 3$. $M^{2+} = Mn^{2+}$; $X^- = ClO_4^-$; $n = 2$. $M^{2+} = Zn^{2+}$; $X^- = NO_3^-$; $n = 2$).

2. Synthesis of imino- and bis-iminopyridine ligands bearing ter-butylaminoxyl groups: radical formation

2.1. Synthesis of the (N-ter-butyl-hydroxyamino)anilines

Bromoanilines were protected in good yields, in two steps according to Weisenfeld [45] (Scheme 1): the monosilylation of the amino group by Me_3SiCl in the presence of Et_3N in a first step was followed by the formation of the amino-Grignard reagent and its condensation with Me_3SiCl.

Hydroxylamines **2b** and **2c** were obtained in 77% and 94% yields, respectively. Oxidation of these derivatives using PbO_2 gave 3-, **3b** and 4-[(*N*-*ter*-butyl-*N*-oxyamino)-*N*,*N*-bis-(trimethylsilyl)]aniline, **3c** (Eq. (1)) (Table 1). In contrast, **1a** reacted with nBuLi but the formed organolithium derivative did not react with 2-methyl-2-nitrosopropane; after hydrolysis, *N*,*N*-bis-trimethylsilylaniline was only obtained.

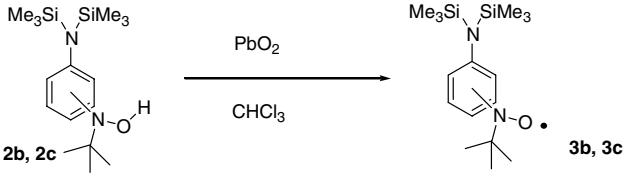

(1)

Unfortunately, when the solutions of **3b** and **3c** are concentrated, they decompose readily; however, the radicals **3b** and **3c** were characterized in the mother liquor using IR, UV and EPR spectroscopy (Table 1). For instance, the IR spectra of **3c** shows the disappearance of the OH bands at 3595 and 3237 cm^{-1} and an intense band at 1359 cm^{-1} attributed to the N–O group [46].

Table 1
Physical properties of the radicals

Radical	UV ($CHCl_3$) nm	IR ($CHCl_3$) cm^{-1}	EPR ($CHCl_3$)
3b	233, 289, 482	1360 (NO)	3 lines $g = 2.0059$ $a_n = 13.1$ G
3c	233, 288, 479	1359 (NO)	3 lines $g = 2.0061$ $a_n = 13.1$ G
5b	230, 293, 484	3460, 3390 (NH_2) 1603 (NH_2) 1363 (NO)	3 lines $g = 2.0053$ $a_n = 13$ G
5c	232, 292, 481	3466, 3389 (NH_2) 1603 (NH_2) 1363 (NO)	3 lines $g = 2.0054$ $a_n = 13$ G
9	230, 291, 379	1361 (NO) 1641 (C=N)	5 lines $g = 2.0054$ $a_{n/2} = 6.7$ G
13	233, 289, 488	1361 (NO) 1641 (C=N)	3 lines $g = 2.0059$ $a_n = 12.5$ G
14	233, 289, 488	361 (NO) 1641 (C=N)	3 lines $g = 2.0057$ $a_n = 13.1$ G
15	230, 291, 345	1364 (NO) 1634 (C=N)	9 lines $g = 2.0036$ $a_{n/2} = 6.0$ G

EPR spectra ($CHCl_3$, $\approx 10^{-5}$ M) were run at room temperature and gave a 1:1:1 triplet due to the coupling of the radical with nitrogen (**3b**: $g = 2$; $a_n = 13.1$ G, **3c**: $g = 2.0061$; $a_n = 13.1$ G). We never observe hyperfine coupling with the hydrogens from butyl and phenyl groups.

The desilylation of the amino group of **2b** and **2c** was performed with aqueous HCl in $CHCl_3$ as solvent. The results are very different depending on the position of the substitution group, *meta* or *para* (Scheme 2). In the case of the *meta* derivative **2b**, deprotection led to the expected 3-(*N*-*ter*-butyl-*N*-hydroxyamino)aniline **4b** in 90% yield. With the *para* derivative **2c**, the deprotection reaction led to a red coloured mixture characteristic of the formation of the aminoxyl radical; this was confirmed by IR and UV measurements and also by the EPR spectrum of the red solution showing three lines

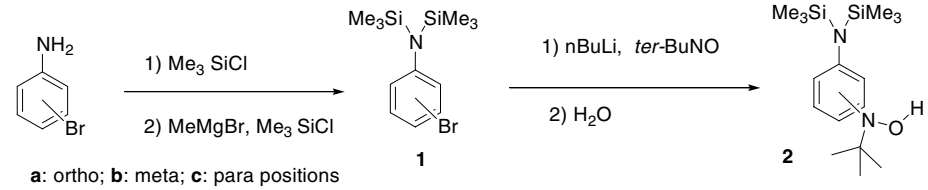

Scheme 1.

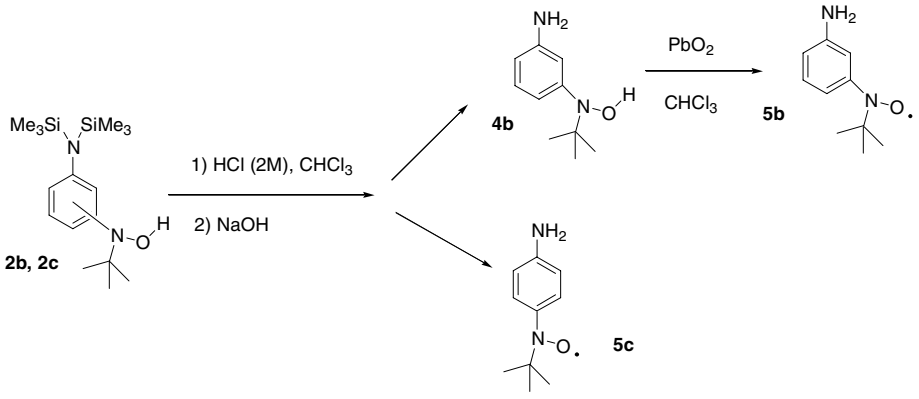

Scheme 2.

at $g = 2.0054$ with $a_N = 13.0$ G (Table 1) which corresponds to **5c**. These values are analogous to those obtained by Rassat et al. [47]; it must be underlined that we were unable to prepare in reasonable yields the *para*hydroxylaniline **4c** using the Grignard procedure of these authors. After filtration and distillation of the solution of **5c**, *N-ter*-butyl-phenyl-1,4-diamine **6c** was obtained in 40% yield: deprotection and oxidation occurred in the same step but decomposition during isolation led to the diamine **6c**.

Oxidation of **4b** led to **5b** which was characterized in solution (Table 1). Indeed, when we tried to isolate **5b** we observed the decomposition of the radical as in the case of **5c**. Radical **5b** gave a mixture of 3-amino-(*N-ter*-butyl)aniline **6b** and the imino quinone **7b** (Eq. (2)).

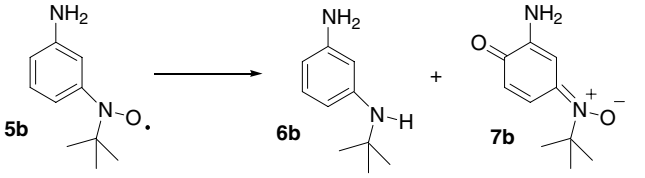

(2)

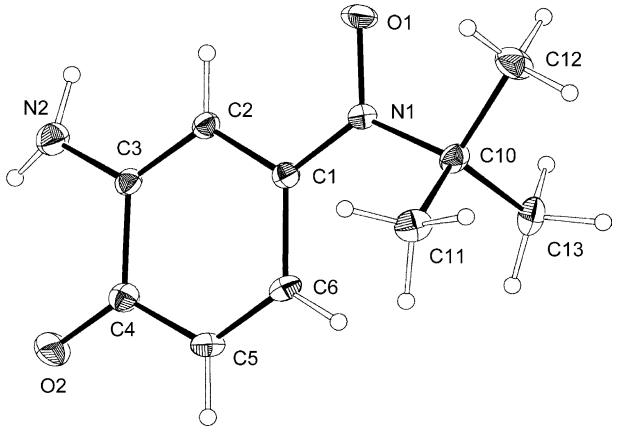

Fig. 1. ORTEP view of **7b**.

Compounds **6b** and **7b** were characterized using ^{1}H NMR, IR and UV spectroscopy. These results are in good accordance with the results obtained by Calder and Forrester in the case of phenyl-*ter*-butylnitroxides

Table 2
Selected bond length (Å) and angles (°) of **7b**

Bond length (Å)	
N1–O1	1.290(5)
N1–C10	1.523(4)
N1–C1	1.359(3)
C1–C2	1.419(3)
C2–C3	1.365(4)
C3–C4	1.487(3)
C4–C5	1.449(4)
C5–C6	1.342(3)
C6–C1	1.448(3)
N2–C3	1.358(3)
O2–C4	1.244(3)
C10–C11	1.531(4)
C10–C12	1.542(4)
C10–C13	1.525(4)
Bonds angles (°)	
C1–N1–O1	118.0(2)
C1–N1–C10	125.6(2)
O1–N1–C10	116.3(2)
N1–C1–C2	119.4(2)
N1–C1–C6	121.3(2)
C6–C1–C2	119.4(2)
C1–C2–C3	121.3(2)
N2–C3–C2	124.2(2)
N2–C3–C4	115.8(2)
C2–C3–C4	120.0(2)
O2–C4–C3	120.5(2)
O2–C4–C5	122.9(2)
C3–C4–C5	116.5(2)
C4–C5–C6	122.5(2)
C5–C6–C1	120.2(2)
N1–C10–C11	11.4(2)
N1–C10–C12	107.2(2)
N1–C10–C13	107.9(2)
C11–C10–C12	108.0(2)
C12–C10–C13	108.4(2)
C13–C10–C11	113.6(2)

[48–50]. Moreover, a red crystal of **7b** was obtained and the structure solved by X-ray analysis. Fig. 1 shows the ORTEP of the crystal structure of **7b** and Table 2 gives selected bond length and angles of **7b**.

The C2–C3 (1.365 Å) and C3–C4 (1.487 Å) distances and the double bond character of C1–N1 (1.359 Å) and C4–O2 (1.244 Å) correspond to a iminoquinone structure, confirmed by the O2–C4–C3 (120.5°) and N1–C1–C6 (121.3°) angles corresponding to sp2 carbons.

In summary, we were able to synthesize the 3-(*N*-*ter*-butyl-*N*-hydroxyamino)aniline **4b** and we shall use it as a synthesis precursor to a new diazabutadiene and to Schiff bases in order to use them as transition metal ligands.

2.2. Synthesis of substituted diazabutadiene and Schiff bases: radical formation

Diazabutadiene, imino- and bis-iminopyridine derivatives are large families of bidentate ligands which are able to coordinate to transition metal [51]. For instance, imino- and bis-iminopyridine derivatives are currently used in the synthesis of, as an example, hydrogenation catalysts prepared by Brookhart et al. [42–44].

The ligands are prepared using the condensation reaction between an amine derivative and a carbonyl compound. We were interested in the preparation of *ter*-butyl aminoxide substituted compounds (Scheme 3).

Diazabutadiene derivatives are easily prepared by the condensation reaction between an amine and glyoxal or butane-2,3-dione; we tried the reaction of the latter with the hydroxylamine **4b** in order to prepare the first aminoxyl-substituted 1,4-diazabutadiene (Scheme 3). The reaction was performed under acidic catalysis, in hexane as solvent, which allowed the precipitation of **8** as soon as formed. Compound **8** is stable under inert atmosphere but it oxidizes slowly in air. Oxidation of **8** with freshly prepared Ag_2O in $CHCl_3$ gave 1,4-bis[3-(*N*-*ter*-butyl-*N*-oxyaminophenyl)]-2,3-dimethyl-1,4-diazabutadiene **9** (Scheme 3).

Compound **9** was characterized using IR, UV, and EPR spectroscopies (Table 1). The IR spectrum shows the disappearance of the OH bands of **8** at 3591 and 3253 cm^{-1}, which demonstrates that the oxidation was complete. The EPR spectrum of **9** shows 5 mains lines with hyperfine coupling for lines 1, 3 and 5 (g = 2.0054, $a_{n/2}$ = 6.7 G). This pattern is consistent with spin exchange between the two unpaired electrons, and with an inter-electronic exchange $J > a_n$ [52]. This interaction is also confirmed by the nitrogen splitting of 6.7 G, that is half of the value observed in the case of a single radical. However, we did not observe any EPR signal

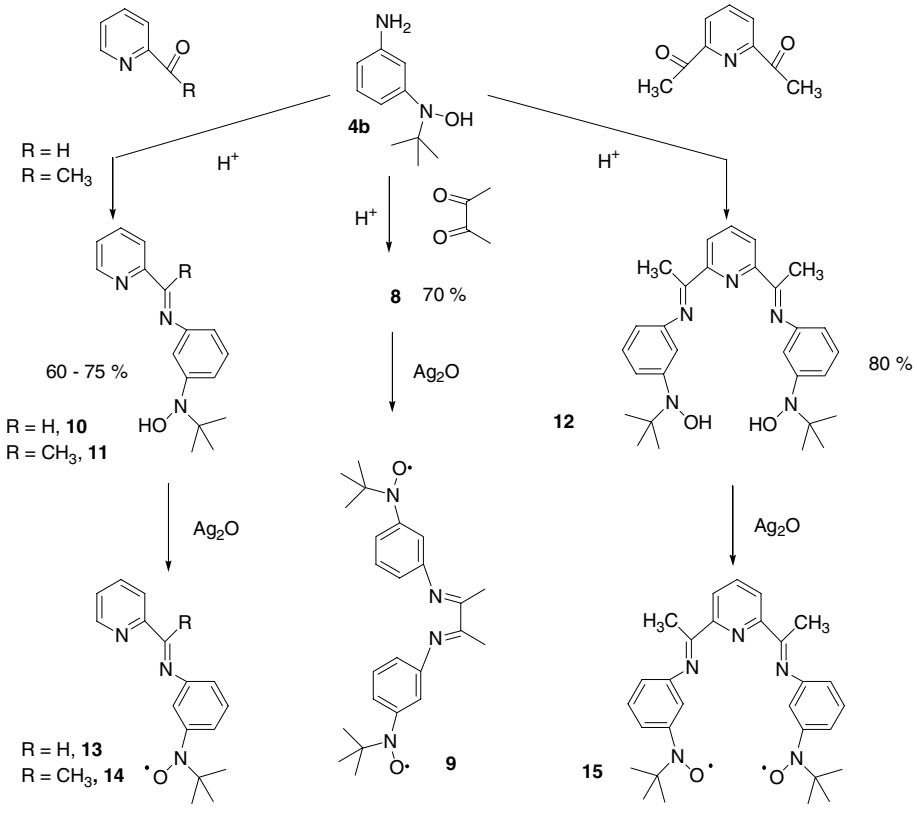

Scheme 3.

corresponding to $\Delta m_s = 2$ at $g = 4$. The hyperfine couplings were fit by spectral simulation [53] as $a_{n/2} = 6.7$, $a_o = 1.7$, $a_m = 0.7$ and $a_p = 1.8$ G. (o, m, p correspond to the hydrogen atoms in *ortho*, *meta* and *para* positions, respectively).

The iminopyridines **10** and **11** and the bis(iminopyridine) **12** were obtained by condensation of amine **4b** with 2-formylpyridine (R = H), 2-acetylpyridine (R = CH_3), and 2,6-diacetylpyridine, respectively. The reactions were performed in refluxing hexane for 72–96 h, under acidic catalysis; this process allowed the precipitation of the derivatives as soon as formed, and the isolation of pure **10**–**12** by filtration, in good yields. These iminopyridines and bis(iminopyridine) are stable under inert atmosphere and were characterized using standard techniques. The oxidation of **10**–**12** was performed in chloroform using freshly prepared Ag_2O and led to **13**–**15** (Scheme 2). The reactions were followed using IR spectroscopy, by the disappearance of the OH bands (3588 and 3242 cm^{-1}). The radicals were analysed using IR, UV and EPR spectroscopies. The results are summarized in Table 1. The infra-red spectra of **13** and **14** show N–O and C=N frequencies at 1361 and 1641 cm^{-1}, respectively, while in **15** these bands are observed at 1364 and 1634 cm^{-1}. The UV spectra of **13**–**15** show the π–π* absorption band of the aminoxyl group at 289 or 291 nm. Finally, EPR spectra of **13** and **14** gave the expected triplet at $g = 2.0059$ with $a_N = 12.5$ G, **13** and $g = 20057$, $a_N = 13.1$ G, **14**. In the case of the bis(iminonitroxide) **15**, the EPR spectrum (Fig. 2) shows 9 lines centred at $g = 2.0036$ with lines 1, 3, 5, 7 and 9 having a hyperfine structure, and lines 1, 2 and 8, 9 being less intense than lines 3, 5 and 7. This EPR spectrum is typical of a diradical with $J \approx a$ [52].

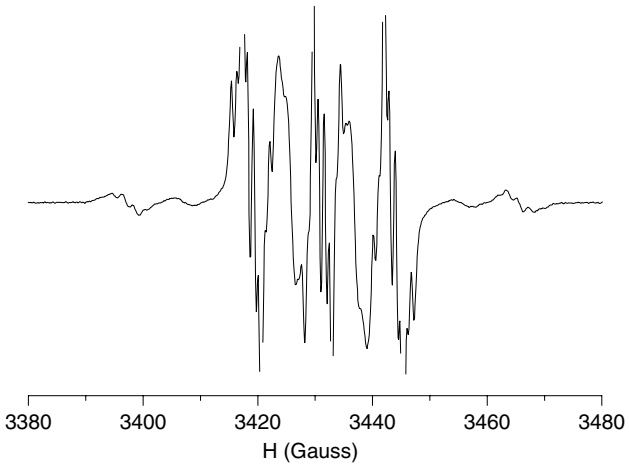

Fig. 2. EPR spectrum of **15**.

As observed in the case of the other radicals (vide supra), **15** is not stable; it decomposes according to Eq. (3). Indeed, column purification gave a red compound characterized as **7b**, already observed in the case of the decomposition of radical **4b**, and diacetylpyridine, identified by NMR.

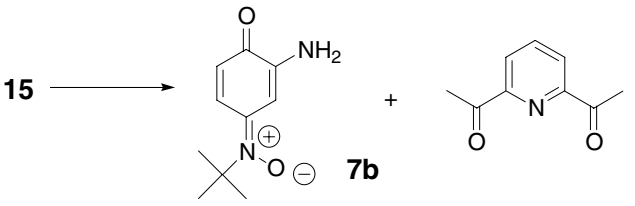

(3)

Table 3
Physical properties of the complexes

Ligand	Metal salt	Complex	IR cm^{-1}	MS FAB$^+$ NBA Mz, intensity
10 L	$NiCl_2 \cdot 4H_2O$	$Ni(L)_2Cl_2 \cdot 1H_2O$	1631	633 [M^+ – Cl, 100]
		16	1361	
	$MnCl_2 \cdot 6H_2O$	$Mn(L)_2Cl_2 \cdot 1H_2O$	1630	628 [M^+ – Cl, 100]
		17	1360	
	$Gd(NO_3)_3 \cdot 5H_2O$	$Gd(L)(NO_3)_3 \cdot 5H_2O$	1638	
		24	1383	
11 L′	$NiCl_24 \cdot H_2O$	$Ni(L')_2Cl_2 \cdot 1H_2O$	1630	659 [M^+ – Cl, 100]
		18	1598	
	$MnCl_2 \cdot 6H_2O$	$Mn(L')_2Cl_2 \cdot 1H_2O$	1633	656 [M^+ – Cl, 100]
		19	1592	
12 L^2	$Zn(NO_3)_2 \cdot 4H_2O$	$Zn(L^2)(NO_3)_2 \cdot 3H_2O$	1638	615 [M^+ – NO_3, 100]
		25	1383	
	$NiCl_2 \cdot 4H_2O$	$Ni(L^2)Cl_2 \cdot 1H_2O$	1626	580 [M^+ – Cl, 100]
		26	1590	
	$MnCl_2 \cdot 6H_2O$	$Mn(L^2)Cl_2 \cdot 1H_2O$	1633	577 [M^+ – Cl, 85]
		27	1592	
	$Mn(ClO_4)_2 \cdot 6H_2O$	$Mn(L^2)_2(ClO_4)_2 \cdot xH_2O$	1629	1129 (M^+ – ClO_4, 38)
		31	1590	1029 (M^+ – $2ClO_4$, 54)
	$Gd(NO_3)_3 \cdot 5H_2O$	$Gd(L^2)(NO_3)_3 \cdot 3H_2O$	1633	769 (M^+ – NO_3, 5)
		32	1383	707 (M^+ – $2NO_3$, 15)

2.3. Complexation of 10, 11, and 12 with M(II) salts (M = Mn, Ni, Zn) and $Gd(NO_3)_3$ and oxidation reactions

The ligands **10**–**12** were synthesized in order to be complexed with transition metals or lanthanides to enhance the total spin number of the molecule. Due to the low stability of the radicals **9**, **13**–**15**, we first prepared the complexes corresponding to the ligands **10**–**12** and oxidized the complexes using freshly prepared Ag_2O. The metals used are: Mn(II), Ni(II), Zn(II) and Gd(III). Table 3 summarizes the observed results.

The complexation reactions of the hydroxylamines **10** and **11** with $NiCl_2$, $MnCl_2$ and $Gd(NO_3)_3$ (using the hydrate salts) were performed under inert atmosphere, in THF as solvent and the complexes were obtained as orange-beige solids in 60–65% yields.

In the case of Ni(II) complexes, the IR spectra show intense bands at 1631 and 1593 cm^{-1} (ν C=N, ν C=C) and 1361 cm^{-1} (ν NO) characteristic of the ligand. Mass spectroscopy and elemental analysis indicated two ligands per metal (Table 3). The complexes **16** and **18** may be described as $Ni(\mathbf{10})_2Cl_2 \cdot 1H_2O$ and $Ni(\mathbf{11})_2Cl_2 \cdot 1H_2O$, respectively. The possible structure is given in Scheme 4 with the chlorine atoms in *trans* positions in order to minimize steric hindrance.

Using $MnCl_2 \cdot 6H_2O$ and **10** and **11**, the two complexes **17** and **19** were obtained. As in the case of the nickel complexes, IR spectra and elemental analysis suggested complexes with two ligands per metal: $Mn(\mathbf{10})_2Cl_2 \cdot 1H_2O$, **17** and $Mn(\mathbf{11})_2Cl_2 \cdot 1H_2O$, **19**, whose must have the structure proposed in the case of the nickel complexes **16** and **18** (Scheme 4).

The oxidation of the nickel complexes **16** and **18** were performed using silver oxide in chloroform as solvent. The oxidized complexes **20** and **22**, at room temperature, gave exactly the same EPR spectra: in chloroform, three lines at $g = 2.0058$ with a hyperfine coupling

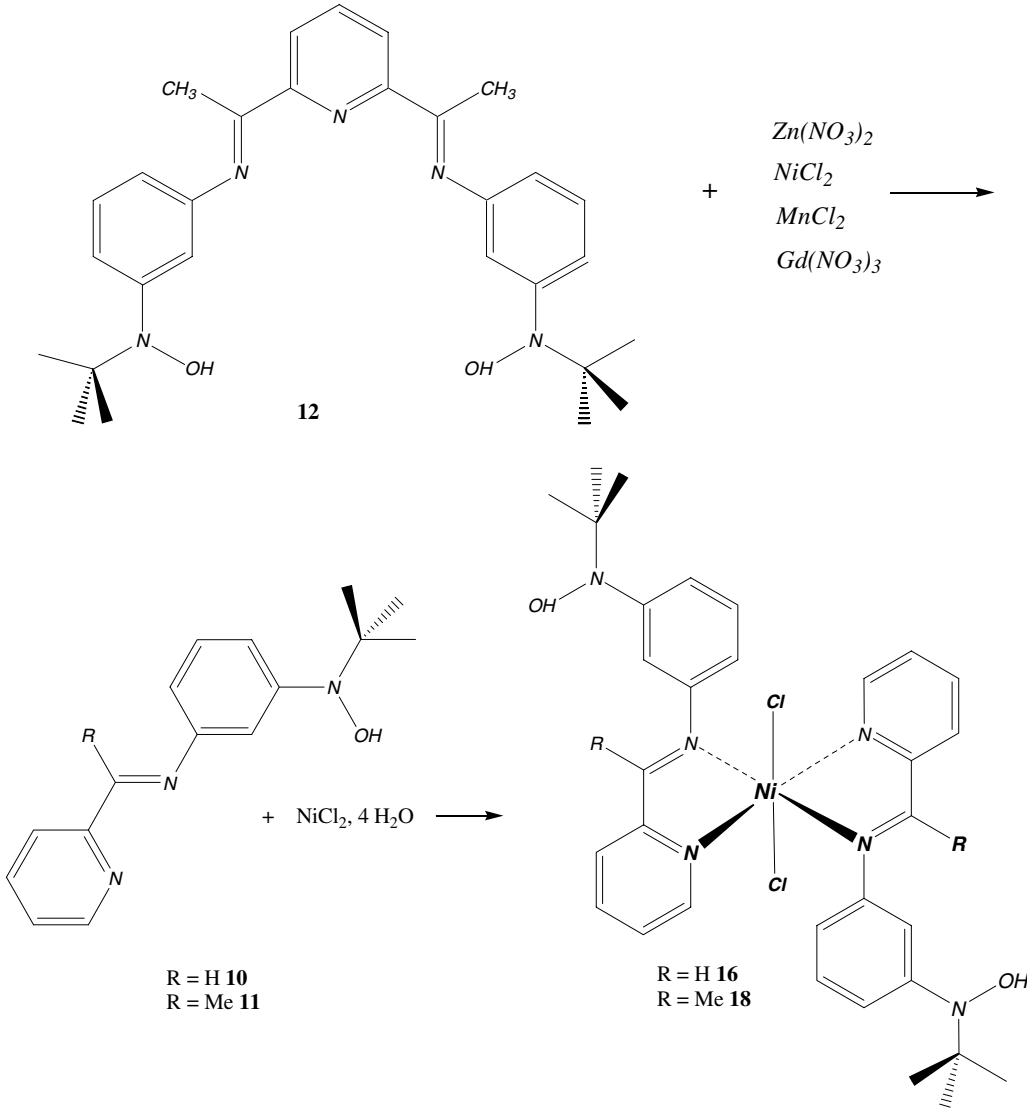

Scheme 4.

constant $a_n = 12.7$ G, characteristic of the aminoxyl group. This pattern demonstrates that there is no coupling between the two aminoxyl radicals. As very often noticed, due to a short relaxation time and a broad signal, the EPR signal of Ni^{2+} was not observed. The solid state EPR spectrum of **20** (or **22**) is shown in Fig. 3; in this case, the signal at $g = 4$, due to the $\Delta m_s = 2$ transition of the NO group, was observed.

The oxidation of **17** and **19** gave the radicals, **21** and **23**, respectively; EPR spectra of **21** and **23** are identical and show a very broad band due to Mn^{2+} and the three lines characteristic of the aminoxyl group. As expected in the case of the latter group, a signal at $g = 4$ was also observed. But, similarly to the nickel complexes **20** and **22**, no coupling was observed between the two radicals of the complex.

In the case of gadolinium, the 1:1 complex obtained with **10** may be written as $Gd(\mathbf{10})(NO_3)_3 \cdot 5H_2O$, **24**. The EPR spectrum of the oxidized complex **24**, prepared using Ag_2O in a 80:20 mixture of chloroform and ethanol, shows the superposition of a broad signal with a peak to peak width of 145 G due to Gd^{3+}, and the three lines at $g = 2.0058$ with $a_n = 12.6$ G of the nitroxide group.

Many complexes with a bis-iminopyridine ligand are known. For instance, Brookhart et al. [54,55]. and Gibson and his group [56] have found that this family of complexes (for instance with cobalt or iron) are very active catalysts in the polymerization of olefins. X-ray analysis of the complexes shows that the metal is pentacoordinated with the three nitrogen in the same plane (Fig. 4).

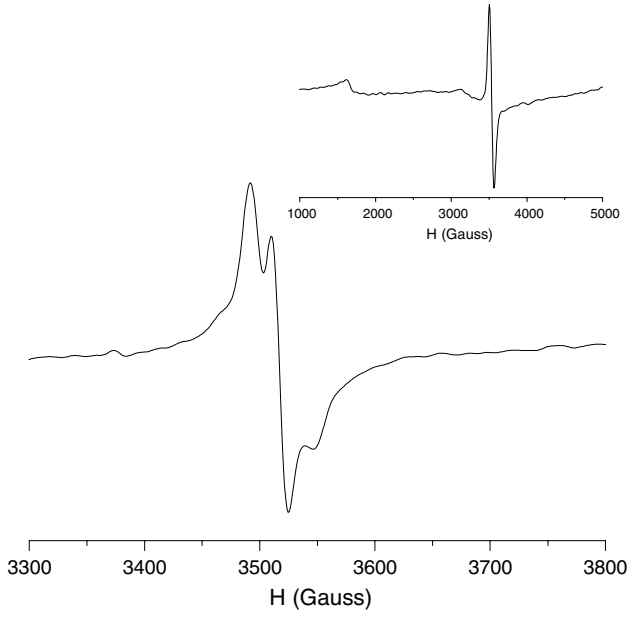

Fig. 3. Solid state, room temperature EPR spectrum of **20** (identical to **22**): (a) around 3500 G; (b) between 1000 and 5000 G.

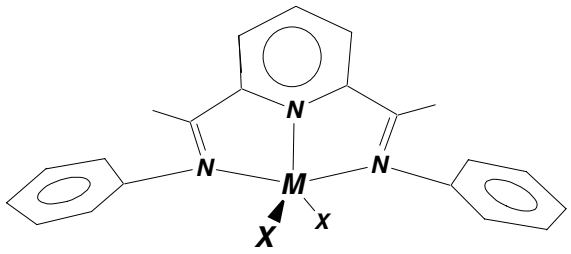

Fig. 4.

In some cases, using different anion X^-, hexacoordinated complexes may be obtained: $[M^{II}(Ligand)_2X_2]$ with $X^- = PF_6^-, ClO_4^-$ or BF_4^-. The latter are octahedral with a distorted square base [57]. In our case, we have studied the complexation of the bis-iminopyridine **12** with different metal salts (Scheme 4).

In order to characterize the complex by NMR, we used $Zn(NO_3)_2$ as a non-paramagnetic metal salt. The reaction was performed in THF at room temperature for 2 h, using $Zn(NO_3)_2 \cdot 4H_2O$ and **12** and the complex **25** was obtained in 65% yield. Elemental analysis and mass spectrum gave a 1:1 metal-to-ligand ratio. The formula of **25** may be written as $Zn(\mathbf{12})\ (NO_3)_2 \cdot 3H_2O$. Infra red spectrum gave the complexed C=N band frequency at 1638 cm^{-1}. In the NMR spectrum, the shifts of the aromatic protons (Fig. 5) demonstrate the formation of the complex. Indeed, in the ligand **12**, the protons of the pyridine group in positions 1 and 2 are situated at 8.1 and 8.45 ppm, and the aromatic protons appeared between 6.6 and 7.3 ppm. After complexation, the pyridine protons are shifted to lower field and appeared as a singlet at 8.75 ppm. Aromatic protons are also shifted of 0.2–0.5 ppm towards lower field. All these results are indicative of a hexacoordinated zinc atom with the three nitrogen atoms of the ligand and two NO_3^- groups, one with monodentate and the second with bidentate coordinations. Oxidation of **25** gave **28** which shows the EPR spectrum of the aminoxyl group, i.e., three sharp lines at $g = 2.0056$ with $a_N = 13$ G.

With $NiCl_2 \cdot 4H_2O$ and **12**, the beige coloured complex **26** was prepared in THF, at room temperature for one hour in 60% yield. IR spectrum gave the ligand bands at 1626 cm^{-1} (C=N), 1590 cm^{-1} (C=C) and 1369 cm^{-1} (NO). The elemental analysis and the mass spectrum indicated a 1:1 metal to ligand ratio. The complex **26** may be described as $Ni(\mathbf{12})Cl_2 \cdot 1H_2O$ with a pentacoordinated structure analogous to that described in Fig. 4. Oxidation of the aminoxyl group using Ag_2O in chloroform gave the complex **29**. EPR spectrum of the latter in solution and at room temperature gave the aminoxyl signal: $g = 2.0056$, $a_N = 12.7$ G. As previously observed, the ESR signal of Ni^{2+} was not observed. Surprisingly, there is no coupling between the two nitroxy radicals; indeed, the oxidized ligand **15** itself gave an EPR spectrum with nine lines (vide supra).

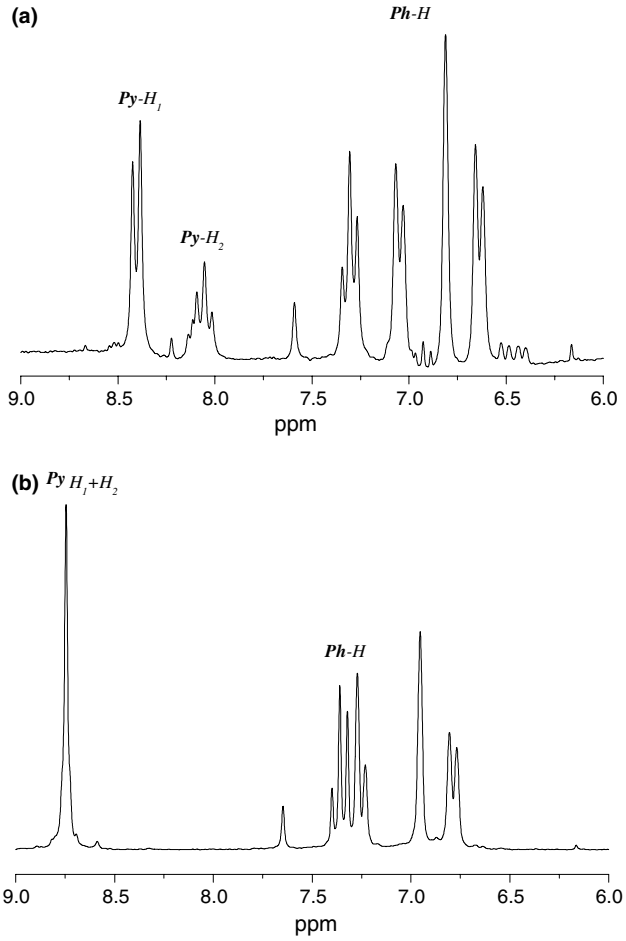

Fig. 5. ^{1}HNMR spectra, aromatic part of: (a) ligand **12**; (b) complex **25**.

An analogous reaction was observed in the case of $MnCl_2 \cdot 6H_2O$. The complex obtained, **27**, may be described as Mn(**12**)$Cl_2 \cdot 1H_2O$ with a pentacoordinated structure (Fig. 4). The oxidation reaction performed with Ag_2O in CH_2Cl_2 as solvent gave complex **30**. EPR spectrum of the latter, in solution and at room temperature, shows the superposition of two signals: one at $g = 2.01$ with six lines corresponding to Mn^{2+} ($S = 5/2$) and the second at $g = 2.007$ with three lines due to the nitroxy group. As observed in the case of the nickel complexe, no interaction was observed between the two radicals of the ligand.

As said previously, hexacoordinated complexes of bis-iminopyridines may be obtained by changing the anion of the metal salt. We have performed the complexation reaction of **12** using $Mn(ClO_4)_2$ as metal(II) salt. Complex **31** was obtained as orange crystals: unfortunately, no crystal was suitable for a X-ray diffraction study was obtained. The mass spectrum indicated a 1:2, metal to ligand ratio; as observed in the literature for related compounds, the Mn^{2+} center must be in a octahedral environment with the perchlorate anions in the outer coordination sphere (Fig. 6).

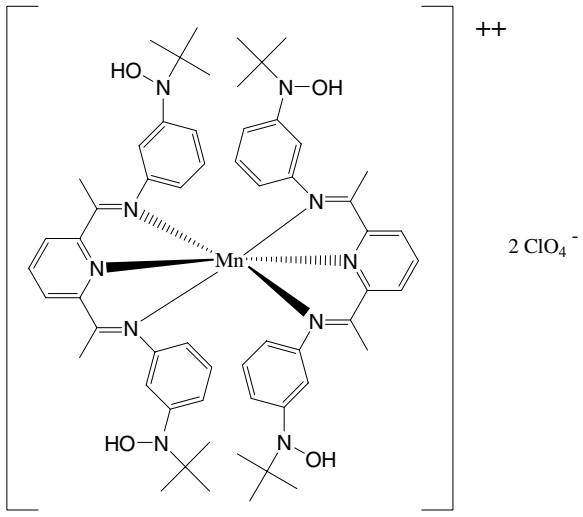

Fig. 6.

The oxidation of **31** was performed in dichloromethane using Ag_2O as oxidation agent and gave **33**. The EPR spectrum of the latter is reproduced in Fig. 7. We were unable to interpret this unexpected shape of this signal.

Using $Gd(NO_3)_3 \cdot 5H_2O$ and the ligand **12**, the red complex **32** was obtained and may be described as Gd(**12**)$(NO_3)_3 \cdot 5H_2O$. The structure of **32** must correspond to a gadolinium atom with eight coordinations, i.e., the three nitrogen atoms, two bidentate and one monodentate NO_3 groups.

The oxidation of **32** using silver oxide in a mixture of THF and ethanol (80:20) gave a red compound; the EPR spectrum in solution, shows the superposition of a broad signal due to Gd^{3+}, and the three lines of a nitroxide group (Table 3).

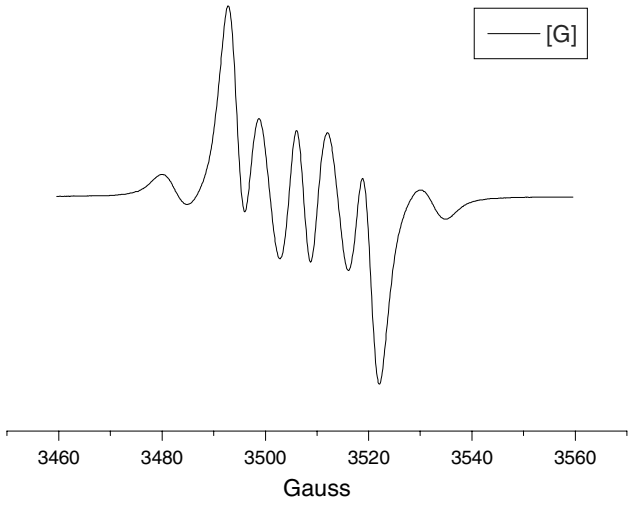

Fig. 7. EPR spectrum of **33**.

3. Conclusion

In conclusion, imino- and bis-iminopyridines bearing one or two N-*ter*-butyl-*N*-hydroxyamino groups, respectively, were prepared. These derivatives were oxidized using PbO_2 to give the *N*-*ter*-butyl-*N*-aminoxyl compounds; the latter were characterized in solution by EPR spectroscopy but, they decompose readily when the solutions are concentrated to give a mixture of amino-(*N*-*ter*-butyl)aniline and an iminoquinone. The latter was characterized by the standard technics and by X-ray diffraction.

These imino- and bis-iminopyridines were used as efficient pincer ligands towards several M^{II}(Mn^{2+}, Ni^{2+}, Zn^{2+}) and Gd^{III} salts giving the corresponding complexes with one or two ligands, depending on the ligand, the metal and the counter anion. The oxidation of the complexes using Ag_2O occurs readily to give the *N*-*ter*-butyl-*N*-aminoxyl derivatives. These complexes were characterized by EPR spectroscopy. In these spectra, the part corresponding to the nitroxide radical are very similar to the oxidized ligands themselves, indicating that there are no interactions between the radicals in the complexes through the metal center.

4. Experimental part

4.1. General

All reactions were carried out under argon or nitrogen using a vacuum line and Schlenk tubes. Solvent were dried and distilled before use. The following compounds were synthesized according to published methods: 4-bromo-*N*-(trimethylsilyl)aniline [45], 4-bromo-*N*,*N*-bis(trimethylsilyl)aniline [45], 2-methyl-2-nitrosopropane [58], 4-(*N*-*ter*-butyl-*N*-oxyamino)aniline [47], 4-*N*-*ter*-butyl-phenyl-1,4-diamine [59], 4-bromo-(*N*-*ter*-butyl-*N*-hy-droxyamino)aniline [60], 4-bromo-(*N*-*ter*-butyl-*N*-*ter*-butyldimethylsilyl)aniline [61]. Ag_2O was prepared using the standard procedure: reaction of $AgNO_3$ with $Ba(OH)_2$. All the metal salts used are hydrates: $NiCl_2 \cdot 4H_2O$; $MnCl_2 \cdot 6H_2O$; $Gd(NO3)_2 \cdot 5H_2O$; $Zn(NO_3)_2 \cdot 4H_2O$; $Mn(ClO_4)_2 \cdot 6H_2O$.

^{1}H NMR spectra were obtained on a Bruker DPX 200; chemical shifts, δ, are relative to TMS. IR spectra were recorded on a Perkin–Elmer 1600 with a 4 cm^{-1} resolution. UV spectra were obtained with a Secaman Anthelie Advanced instrument using quartz cells (∅1 cm); wave lengths are in nm. Mass spectra were recorded on a Jeol JMS D300 using electronic impact (EI), or Fast Atom Bombardment in the positive (FAB^+) or negative (FAB^-) modes with 3-nitro-benzyl alcohol (NBA) or thioglycerol (GT) as matrixes. EPR spectra were recorded on a Bruker 500 (X-band) using standard EPR tubes in degassed solvent; concentration range: 10^{-5}–10^{-6} mole/L.

4.2. Crystal data for **7b**

Nonius CAD 4 automated diffractometer, crystal of dimensions $0.30 \times 0.10 \times 0.06$ m^3 mounted on a glass fiber with mineral oil at 173 K. $C_{10}H_{14}N_2O_2$, $M = 194.23$, monoclinic, space group $P2_1/c$, $a = 10.490(4)$, $b = 8.061(21)$, $c = 11.689(2)$ Å, $\beta = 95.67(2)°$, $V = 983.6(26)$ $Å^3$, $D_{calc.} = 1.312$, $T = 170$ K, $Z = 4$, F (000) = 416, μMo Kα = 0.09 mm^{-1}, 2541 reflections measured, 2311 unique ($R_{int} = 0.0532$) which were used in all calculations. The structure was solved by direct methods using SHELXS 86 [62], and refined by least- squares on F^2 with the help of SHELXL 93 [63]. The hydrogen atoms on the aromatic ring and the *t*-butyl were positioned by calculation [63]. The hydrogen atoms on N2 were revealed on a difference Fourier map and their coordinates were fixed throught the subsequent refinement cycles. The final $R(F)$ value was 0.0435 for 869 $F_o > 4s(F_o)$ and $wR(F^2) = 0.0762$.

Safety note: Although we have experienced no problems, perchlorate salts are potentially explosive. They should be handled with extreme care and used only in small quantities without heat. [64,65]

4.3. 3-, and 4-(N-ter-butyl-N-hydroxyamino)-N,N-bis(trimethylsilyl)aniline **2b**, and **2c**

A solution of BuLi (2,2 M, 25 mL, 55 mmol) was added dropwise to a solution of **1b** or **1c** (17 g, 54 mmol.) in 150 mL diethylether at −20 °C and the mixture was stirred for 1 h at that temperature. A solution of 2-methyl-2-nitrosopropane (5 g, 57 mmol) in 60 mL of diethylether was added dropwise in 10 min to the reaction mixture at 0 °C. The mixture was allowed to reach room temperature and stirred for 1 h. After hydrolysis at 0 °C and standard work-up, the residue was crystallized from pentane to give a white crystalline powder.

4.3.1. Compound **2b**

Yield: 77%, m.p. = 179–181 °C. IR (CCl_4), ν (cm^{-1}): 3589, 3236 (OH), 1360 (N–OH), 1247 ($SiMe_3$). ^{1}H NMR ($CDCl_3$), δ (ppm): 0.08 (s, 18 H, $SiMe_3$), 1.24 (s, 9 H, *ter*-Bu), 6.68–7.35 (m, 4H, Ar). MS (FAB^+, NBA) (*m*/*z*, intensity): 325 (M^+, 60), 252 ($M^+ - SiMe_3$, 50), 73 ($SiMe_3^+$, 100). Anal. Calc. for $C_{16}H_{32}N_2OSi_2$: C, 59.20; H, 9.94; N, 8.63. Found: C, 58.84; H, 9.93; N, 8.50%.

4.3.2. Compound **2c**

Yield: 94%, m.p. = 176–178 °C. IR (CCl_4), ν (cm^{-1}): 3595, 3237 (OH), 1348 (N–OH), 1249 ($SiMe_3$). ^{1}H NMR ($CDCl_3$), (ppm): 0.07 (s, 18H, $SiMe_3$), 1.07 (s, 9 H, *ter*-Bu), 6.81 (d, 2H, $^3J_{HH} = 7.9$ Hz), 7.35 (d, 2H,

$^3J_{HH}$ = 7.9 Hz). MS (FAB$^+$, NBA) (*m*/*z*, intensity): 323 ($M^+ - H$, 30), 267 ($M^+ -$ *ter*-Bu, 90), 251 ($M^+ - SiMe_3$, 95), 73 ($SiMe_3^+$, 100). Anal. Calc. for $C_{16}H_{32}N_2OSi_2$: C, 59.20; H, 9.94; N, 8.63. Found: C, 58.77; H, 9.85; N, 8.45%.

4.3.3. Compound **2a**

No reaction was observed, using the same procedure, between the lithium derivative of **1a** and 2-methyl-2-nitrosopropane. After hydrolysis, *N*,*N*-bis(trimethylsilyl)aniline was obtained in 97% yield.

4.4. 3- and 4-(*N*-ter-butyl-*N*-oxyamino)-*N*,*N*-bis(trimethylsilyl)aniline **3b** and **3c**

PbO_2 (1.2 g, 5 mmol) was added to a solution of **2b** or **2c** (0.52 g, 1.6 mmol) in 50 mL of $CHCl_3$. The mixture was vigorously stirred for 25 min (up to the disparition of the OH band in IR spectroscopy). The red solution was filtrated using celite and all analyses were performed on this solution, without evaporation.

4.4.1. Compound **3b**

IR (CCl_4), ν (cm^{-1}): 1360 (N–O), 1247, 970 ($SiMe_3$). EPR ($CHCl_3$): three lines at g = 2.0059, a_N = 13.1 G. UV ($CHCl_3$), λ nm: 233 (π–π* Ph), 289 (π–π* N–O), 482 (n–π* N–O).

4.4.2. Compound **3c**

IR (CCl_4), ν (cm^{-1}): 1359 (N–O), 1249, 974 ($SiMe_3$). EPR ($CHCl_3$): three lines at g = 2.0061, a_N = 13.1 G. UV ($CHCl_3$), λ nm: 233 (π-π* Ph), 288 (π–π* N–O), 479 (n–π* N–O).

4.5. 3-(*N*-ter-butyl-*N*-hydroxyamino)aniline **4b**

A deoxygenated water solution of HCl 4M (40 mL, 0.16 mol) was added dropwise to a ethereal solution (25 mL) of **3b** (6.3 g, 20 mmol) and the mixture was stirred vigorously for 5 min under inert atmosphere. After phases separation and extraction of the water phase with diethylether, a solution of NaOH (4 M solution, 40 mL, 0.16 mmol) was added dropwise to the ethereal solution under vigorous stirring. The organic phase was separated, dried over $MgSO_4$ and the solvent was removed under vacuum to leave a white powder; recrystallization from pentane gave **4b** in 90% yield. m.p. 130–133 °C. IR (CCl_4), ν (cm^{-1}): 3587, 3219 (OH), 3479, 3389 (NH_2). ^{1}H NMR ($CDCl_3$), δ (ppm): 1.16 (s, 9H, *ter*-Bu), 2.08 (s, 2H, NH_2), 6.47–6.53 (m, 1H, C5–H), 6.63–6.68 (m, 2 H, C4- and C6–H), 7.02–7.11 (m, 1H, C2–H). ^{13}C NMR ($CDCl_3$), δ (ppm): 26.5 (*C*H$_3$), 61 (*C*–CH$_3$), 112 (*C2*), 113 (*C6*), 115 (*C4*), 128 (*C5*), 146 (*C3*), 150 (*C1*). MS (FAB$^+$, NBA) (*m*/*z*, intensity): 181 ($M + 1^+$, 100), 124 ($M^+ -$ *ter*-Bu, 35). Anal. Calc. for $C_{10}H_{16}N_2O$: C, 66.64; H, 8.95; N, 15.54. Found: C, 67.21; H, 8.83; N, 15.61%.

4.6. Deprotection of **3c** and oxidation

A water solution of HCl (3 M, 10 mL, 6 mmol) was added dropwise to a solution of **3c** (1.9 g, 6 mmol) in chloroform (25 mL) and the mixture was stirred for 30 min. After phase separation, chloroform, 50 mL, was added to the water phase and, under stirring a NaOH solution (3 M, 11 mL, 33 mmol) was added dropwise up to a pH of 8. The organic phase was separated and dried over $MgSO_4 \cdot PbO_2$ (3 g, 12 mmol) was added, stirred for 30 min and the red solution was filtered over celite. All the analysis were done using this chloroform solution. IR ($CHCl_3$), ν (cm^{-1}): 3466, 3389 and 1603 (NH_2), 1363 (N–O). EPR ($CHCl_3$): g = 2.0054, 3 lines a_N = 13 G. UV ($CHCl_3$), λ nm: 232 (π–π* Ph), 292 (π–π* N–O), 481 (n–π* N–O).

The chloroform solution was evaporated under vacuum and the residue distillated (80 °C, 0.1 Torr) to give an orange oil with 40% yield (0.4 g, 2.4 mmol). The compound was characterized as 4-*N*-*ter*-butyl-phenyl-1,4-diamine. IR (CCl_4), ν (cm^{-1}): 3461, 3384 (NH, NH_2). ^{1}H NMR ($CDCl_3$), δ (ppm): 1.23 (s, 9H, CH_3), 3.25 (s, 3H, NH), 6.61 (d, 2H, $^3J_{HH}$ = 8.1 Hz, Ar), 6.77 (d, 2H,$^3J_{HH}$ = 8.1 Hz, Ar). MS (FAB$^+$, NBA) (*m*/*z*, intensity): 164 (M^+, 100), 149 ($M^+ - CH_3$, 40).

4.7. 3-(*N*-ter-butyl-*N*-oxyamino)aniline **5b**

PbO_2 (2.4 g, 10 mmol) was added to a solution of **4b** (1.2 g, 3.7 mmol) in chloroform (60 mL) under stirring. The reaction was followed using IR spectroscopy; after 10 min the OH bands have disappeared. The red solution was filtered over celite and all analysis were done on that solution. IR ($CHCl_3$), ν (cm^{-1}): 3460, 3390 and 1597 (NH_2), 137 (N–O). EPR ($CHCl_3$): g = 2.0053, 3 lines a_N = 13.2 G. UV ($CHCl_3$), λ nm: 230 (π–π* Ph), 293 (π–π* N–O), 484 (n–π* N–O).

4.8. Decomposition of 3-(*N*-ter-butyl-*N*-oxyamino)aniline **5b**: characterization of 3-amino-(*N*-ter-butyl)aniline **6b** and quinone **7b**

The solution of **5b** was dried under vacuum and the residue dissolved in diethylether and chromatographed over silica. A red compound was obtained after evaporation of the solvent. Recrystallization from diethylether; m.p. 99–101 °C. IR ($CHCl_3$), ν (cm^{-1}): 3477, 3352 and 1585 (NH_2), 1630 (C=O). ^{1}H NMR ($CDCl_3$), δ (ppm): 7.75 (dd, 1H, J = 3 Hz, J = 10 Hz), 6.9 (d, 1H, J = 3 Hz), 6.3 (d, 1H, J = 10 Hz), 4.6 (broad, 2H, NH_2), 1.75 (s, 9H, *ter*-Bu). MS (FAB$^+$, NBA) (*m*/*z*, intensity): 195 ($M^+ + 1$, 5), 139 ($M^+ -$ *ter*-Bu, 100). IR and NMR values are similar to the values observed in the case of

N-ter-butylated imino quinone 3-(*ter*-butylamino)-*N-ter*-butyl-1,4-benzoquinone imine *N*-oxide [66]. See Table 2 and Fig. 1 for X-ray analysis.

4.9. 1,4-bis-[3-(N-ter-butyl-N-hydroxyamino)phenyl]-2,3-dimethyl-1,4-diazabutadiene **8**

A mixture of 2,3-butanedione (0.35 g, 4 mmol) and **4b** in hexane (80 mL) was heated under reflux in a Dean Stark apparatus for 30 h, with a few drops of acetic acid to catalyze the reaction. Precipitation of **8** occurred during the reaction. The mixture was cooled to 0 °C, filtered and the solid washed two times with 30 mL of cold hexane. **8** was obtained as a brown-grey powder with 70% yield. m.p. 148–151 °C (dec.). IR (CCl_4), ν (cm^{-1}): 3591,3253 (OH), 1641 (C=N). ^1H NMR ($CDCl_3$), δ (ppm): 1.12 (s, 18H, *ter*-Bu), 2.13 (s, 6H, CH_3), 6.57-6.94 (m, 2H, C5–H), 7.04–7.15 (m, 4H, C4–H and C6–H), 7.23–7.52 (m, 2H, C2–H). MS (FAB^+, NBA) (*m/z*, intensity): 411 ($M^+ + H$, 25), 57 (*ter*-Bu, 100).

4.10. 1,4-bis-[3-(N-ter-butyl-N-oxyamino)phenyl]-2,3-dimethyl-1,4-diazabutadiene **9**

PbO_2 (2.4 g, 10 mmol) was added to a chloroform solution (60 mL) of **8** (1.5 g, 3.6 mmol). The mixture was stirred vigorously for 5 min (disappearance of the OH bands in IR spectroscopy). The red solution was filtered using celite and the analysis were done on this solution. IR ($CHCl_3$), ν (cm^{-1}): 1641 (C=N), 1361 (N–O). EPR ($CHCl_3$): $g = 2.0036$, 5 principal lines; $a_N = 6.7$ G, $a_H = 1.7$ (Ho), 0.7 (Hm), 1.8 (Hp). UV ($CHCl_3$), λ nm: 230 (π–π* Ph), 291 (π–π* N–O), 379 (π* N=C–C=N).

4.11. N-[3-(N-ter-butyl-N-hydroxyaminophenyl)]-(2-pyridyl)methanimine **10** and N-[3-(N-ter-butyl-N-hydroxyaminophenyl)]-(2-pyridyl)ethanimine **11**

Same procedure as for **8** but 72 h reaction for **10** and 96 h in the case of **11**.

4.11.1. Compound **10**

Yield: 75%, m.p. 78–81 (dec.). IR (CCl_4), ν (cm^{-1}): 3588, 3242 (OH), 1631 (C=N). ^1H NMR ($CDCl_3$), δ (ppm): 1.25 (s, 9 H, *ter*-Bu), 6.0 (s, br, 1H, OH), 7.05–7.32 (m, 4H, Ar), 7.41 (m, 1H, Py C5-H), 7.84 (m, 1 H, Py C3–H or C4–H), 8.22 (m, 1H, Py C3–H or C4–H), 8.63 (s, 1H, N=C–H), 8.75 (m, 1H, Py C6–H). MS (FAB^+, NBA) (*m/z*, intensity):270 (M^+, 100), 213 ($M^+ -$ *ter*-Bu, 40), 57 (*ter*-Bu^+, 50).

4.11.2. Compound **11**

Yield: 60%, m.p. 119–122 (dec). IR (CCl_4), ν (cm^{-1}): 3592, 3281 (OH), 1643 (C=N). ^1H NMR ($CDCl_3$), δ (ppm): 1.18 (s, 9H, *ter*-Bu), 2.36 (s, 3H, N=C–CH_3), 6.62–7.32 (m, 4H, Ar), 7.41 (m, 1H, Py C5–H), 7.82 (m, 1H, Py C3–H or C4–H), 8.28 (m, 1H, Py C4–H or C3–H), 8.70 (m, 1H, Py C6–H). MS (FAB^+, NBA) (*m/z*, intensity):284 (M^+, 50), 267 ($M^+ -$ OH, 50), 57 (*ter*-Bu^+, 100).

4.12. N-[3-(N-ter-butyl-N-oxyaminophenyl)]-(2-pyridyl)methanimine **13** and N-[3-(N-ter-butyl-N-oxyaminophenyl)]-(2-pyridyl)ethanimine **14**

Same procedure as for **9**.

4.12.1. Compound **13** and **14**

IR ($CHCl_3$), ν (cm^{-1}): 1641 (C=N), 1361 (N–O). UV ($CHCl_3$), λ nm: 233 (π–π* Ph), 289 (π–π* N–O), 488 (n–π* N–O). **13**: EPR ($CHCl_3$): $g = 2.0059$, 3 lines, $a_N = 12.5$ G. **14**: EPR ($CHCl_3$): $g = 2.0057$, 3 lines $a_N = 13.1$.

4.13. bis-{1-[3-(N-ter-butyl-N-hydroxyamino)phenylimino]ethyl} pyridine **12**

Same procedure as for **8**. **12**: Yield: 80%. m.p. 212–214 °C (dec). IR (KBr), ν (cm^{-1}): 3242 (OH), 1638 (C=N). ^1H NMR ($CDCl_3$), δ (ppm): 1.20 (s, 18H, *ter*-Bu), 2.41 (s, 6H, CH_3), 6.10 (s, br, 2H, OH), 6.68 (dt, 2H, 7.7 and 1 Hz, Ph C4–H or C6–H), 6.78 (t, 2H, 2 Hz, Ph C2–H), 7.04 (dt, 2H, 7.7 and 1 Hz, Ph C4–H or C6–H), 7.30 (t, 2H, 7.9 Hz, Ph C5–H), 7.89 (t, 1H, 7.6 Hz, Py C4–H), 8.35 (d, 2H, 7.8 Hz, Py C3–H and C5–H). MS (FAB^+, NBA) (*m/z*, intensity):488 ($M^+ + H$, 50), 472 ($M^+ -$ OH, 10), 57 (*ter*-Bu^+, 100). Anal. Calc. for $C_{29}H_{37}N_5O_2$: C, 71.43; H, 7.65; N, 14.36; O, 6.56. Found: C, 70.99; H, 7.54; N, 13.85; O, 6.65%.

4.14. bis-{1-[3-(N-ter-butyl-N-oxyamino)phenylimino]ethyl} pyridine **15**

Same procedure as for **9**. IR ($CHCl_3$), ν (cm^{-1}): 1634 (C=N), 1364 (N–O). EPR (see text and Table 3). UV ($CHCl_3$), λ nm: 230 (π–π* Ph), 291 (π–π* N–O), 345 (π–π* N=C–C=N).

5. Complexation reactions

5.1. General procedure

The metal salt was dissolved in THF and added dropwise to a solution of the ligand (1.05 equiv.) in THF, under inert atmosphere. The reaction mixture was stirred for 1 h (case of the ligand **11** and **12**) or several hours (case of **15**) and evaporated under vacuum. Addition of diethylether left a solid which was washed several times with diethylether and pentane. The solids were dried under vacuum.

5.2. Case of ligands **10** and **11**

5.2.1. Dichloro-bis-2-[3-N-ter-butyl-N-hydroxyaminopyridin-2-yl-methylene-phenylamine]nickel(II), **16**

Orange-beige powder; Yield: 72% dec. > 260 °C. IR (KBr), ν (cm^{-1}): 3242 (OH), 1631 (C=N), 1593 (C=C). MS (FAB^+, NBA), *m/z* (intensity): 633 ($M^+ - Cl$, 100), 596 ($M^+ - 2Cl$, 100), 57 (*ter*-Bu^+, 100). Anal. Calc. for Ni(**10**)$_2Cl_2 \cdot 1H_2O$, $C_{32}H_{40}Cl_2N_6NiO_3$: C, 56.00; H, 5.87; N, 12.25. Found: C, 56.55; H, 6.14; N, 12.22%.

5.2.2. Dichloro-bis-2-[3-N-ter-butyl-N-hydroxyamino-(1-pyridin-2-yl-ethyl) phenylamine]nickel(II), **18**

Orange-beige powder; Yield: 75%, dec. > 260 °C. IR (KBr), ν (cm^{-1}): 3242 (OH), 1629 (C=N). MS (FAB^+, NBA), *m/z* (intensity): 659 ($M^+ - Cl$, 100), 624 ($M^+ - 2Cl$, 70), 57 (*ter*-Bu^+, 40). Anal. Calc. for Ni(**11**)$_2Cl_2 \cdot 1H_2O$, $C_{34}H_{44}Cl_2N_6NiO_3$: C, 57.16; H, 6.21; N, 11.76. Found: C, 57.00; H, 6.31; N, 11.39%.

5.2.3. Dichloro-bis-2-[3-N-ter-butyl-N-hydroxyaminopyridin-2-yl- methylene-phenylamine]manganese(II), **17**

Orange-beige powder; Yield: 80% dec. > 250 °C. IR (KBr), ν (cm^{-1}): 3400 (OH), 1655 (C=N). MS (FAB^+, NBA), *m/z* (intensity): 628 ($M^+ - Cl$, 100), 57 (*ter*-Bu^+, 55). Anal. Calc. for Mn(**10**)$_2Cl_2 \cdot 1H_2O$, $C_{32}H_{40}Cl_2MnN_6O_3$: C, 56.31; H, 5.91; N, 12.31. Found: C, 57.82; H, 5.56; N, 11.66%.

5.2.4. Dichloro-bis-2-[3-N-ter-butyl-N-hydroxyamino-(1-pyridin-2-yl-ethyl) phenylamine]manganese(II), **19**

Orange-beige powder; Yield: 69%, dec. > 260 °C. IR (KBr), ν (cm^{-1}): 3330 (OH), 1633 (C=N). MS (FAB^+, NBA), *m/z* (intensity): 656 ($M^+ - Cl$, 100), 621 ($M^+ - 2Cl$, 45), 57 (*ter*-Bu^+, 55). Anal. Calc. for Mn(**11**)$_2Cl_2 \cdot 2H_2O$, $C_{34}H_{46}Cl_2MnN_6O_4$: C, 56.05; H, 6.36; N, 11.53. Found: C, 56.42; H, 6.94; N, 11.40%.

5.2.5. Trinitro-2-[3-N-ter-butyl-N-hydroxyaminopyridin-2-yl- methylene-phenylamine]gadolinium(III), **24**

Orange-beige powder; Yield: 57%, dec. > 230 °C. IR (KBr), ν (cm^{-1}): 3392 (OH), 1638 (C=N), 1383 (NO_3). Anal. Calc. for Gd(**10**)$(NO_3)_3 \cdot 5H_2O$, $C_{16}H_{29}GdN_6O_{15}$: C, 27.35; H, 4.16; N, 11.96. Found: C, 27.45; H, 3.66; N, 11.52%.

5.3. Case of ligand **12**

5.3.1. Dinitro-2,6bis-[1-(3-N-ter-butyl-hydroxylamino-phenylimino)ethyl]pyridine zinc(II), **25**

Orange-beige powder; Yield: 65%, dec.: > 280 °C. IR (KBr), ν (cm^{-1}): 3392 (OH), 1638 (C=N), 1383 (NO_3). ^1H NMR (acetone d_6) δ (ppm, Hz): 1.17 (s, 18H, N-*ter*-Bu), 2.72 (s, 6H, =C(CH_3)), 6.78 (d, 2H, 6.9 Hz, Ph), 6.95 (s, 2H, Ph), 7.23–7.40 (m, 4H, Ph), 8.75 (s, 3H, Py). MS (FAB^+, NBA), *m/z* (intensity):615 ($M^+ - NO_3$, 100); 555 ($M^+ - 2NO_3$, 15), 57 (*ter*-Bu^+, 35). Anal. Calc. for Zn(**12**)$(NO_3)_2 \cdot 3H_2O$, $C_{29}H_{41}N_7O_{11}Zn$: C, 47.65; H, 5.93; N, 13.40. Found: C, 47.65; H, 5.92; N, 12.83%.

5.3.2. Dichloro-2,6bis-[1-(3-N-ter-butyl-hydroxylamino-phenylimino)ethyl]pyridine nickel(II), **26**

Orange-beige powder; Yield: 60%, dec. > 280 °C. IR (KBr), ν (cm^{-1}): 3348 (OH), 1627 (C=N). MS (FAB^+, NBA), *m/z* (intensity):580 ($M^+ - Cl$, 100); 57 (*ter*-Bu^+, 80). Anal. Calc. for Ni(**12**)$Cl_2 \cdot 1H_2O$, $C_{29}H_{39}Cl_2N_5NiO_3$: C, 54.82; H, 6.19; N, 11.02. Found: C, 55.55; H, 6.04; N, 10.57%.

5.3.3. Dichloro-2,6bis-[1-(3-N-ter-butyl-hydroxylamino-phenylimino)ethyl]pyridine manganese(II), **27**

Beige powder; Yield: 65%, dec. > 280 °C. IR (KBr), ν (cm^{-1}): 3378 (OH), 1633 (C=N). MS (FAB^+, NBA), *m/z* (intensity):577 ($M^+ - Cl$, 85); 545 ($M^+ - 2Cl$, 15);488 ($M^+ - 2Cl$-*ter*-Bu, 35); 57 (*ter*-Bu^+, 35). Anal. Calc. for Mn(**12**)$Cl_2 \cdot 3H_2O$, $C_{29}H_{46}Cl_2MnN_5O_5$: C, 52.17; H, 6.49; N, 10.48. Found: C, 52.93; H, 5.72; N, 10.44%.

5.3.4. Diperchlorato-2,6bis-[1-(3-N-ter-butyl-hydroxyl-aminophenylimino)ethyl]pyridine manganese(II), **31**

Orange crystals. m.p. > 120 °C (the complex was not heated more than that temperature). (No X-ray diffraction pattern was obtained). IR (KBr), ν (cm^{-1}): 3442 (OH), 1629 (C=N), 1101, 950 (ClO_4). MS (FAB^+, NBA), *m/z* (intensity):1129 ($M^+ - ClO_4$, 38); 1029 ($M^+ - 2ClO_4$, 52).

5.3.5. Trinitro-2,6bis-[1-(3-N-ter-butyl-hydroxylamino-phenylimino)ethyl]pyridine gadolinium(III), **32**

Beige powder. Yield: 65%, $T_{dec.}$ > 280 °C. IR (KBr), ν (cm^{-1}): 3378 (OH), 1633 (C=N), 1383 (NO_3). MS (FAB^+, NBA), *m/z* (intensity): 769 ($M^+ - NO_3$, 5); 707 ($M^+ - 2NO_3$, 15); 650 ($M^+ - 2NO_3$-*ter*-Bu, 60). Anal. Calc. for Gd(**12**)$(NO_3)_3 \cdot 3H_2O$, $C_{29}H_{43}GdN_8O_{14}$: C, 39.36; H, 4.90; N, 12.66. Found: C, 39.38; H, 4.72; N, 11.90%.

5.4. Oxidation of the complexes

5.4.1. General procedure

Ag_2O (2 equiv.) was added to a solution of the complex in chloroform and the mixture was stirred at room temperature for 30 mn. After filtration over celite, the solution was evaporated and the obtained solid was dried under vacuum.

5.4.2. Oxidation of **25**

EPR spectrum of **28** was run in $CHCl_3$, after filtration over celite. $g = 2.0056$, $a_N = 13$ G.

*5.4.3. Oxidation of **26***

Complex **29** was obtained as a red powder. Yield: 90%, EPR: see Table 3. IR (KBr), ν (cm^{-1}): 3348 (OH), 1627 (C=N). Anal. Calc. for Ni(**15**)$Cl_2 \cdot 2H_2O$, $C_{29}H_{39}Cl_2N_5NiO_4$: C, 53.48 H, 6.03; N, 10.74. Found: C, 53.55; H, 6.91; N, 10.57%.

*5.4.4. Oxidation of **27***

Complex **30** was obtained as a red powder. Yield: 95%, EPR: see Table 3. IR (KBr), ν (cm^{-1}): 3378 (OH), 1633 (C=N). Anal. Calc. for Mn(**15**)$Cl_2 \cdot 2H_2O$, $C_{29}H_{39}Cl_2MnN_5O_4$: C, 53.79 H, 6.07; N, 10.81. Found: C, 52.93; H, 5.72; N, 10.44%.

*5.4.5. Oxidation of **31***

The red solution of complex **33**, after filtration on celite was characterized using EPR spectroscopy. See Table 3 and Fig. 6. Thin layer chromatography (TLC) with CH_2Cl_2 led to partial decomposition: 3 spots were obtained but the best migrating red spot has the same spectrum as the initial solution. This seams to indicate that the latter corresponds to a single complex.

*5.4.6. Oxidation of **32***

Complex **34** was obtained as a red powder. Yield: 93%, EPR: see Table 3. IR (KBr), ν (cm^{-1}): 3378 (OH), 1633 (C=N), 1383 (NO_3). Anal. Calc. for Gd(**15**)$(NO_3) \cdot 3H_2O$, $C_{29}H_{41}GdN_8O_{14}$: C, 39.45; H, 4.68; N, 12.68. Found: C, 39.26; H, 4.68; N, 11.85%.

6. Supporting information available

Crystallographic data for the structural analysis have been deposited with the Cambridge Crystallographic Data Center, CCDC No. 238906. Copies of this information may be obtained free of charge from The Director, CCDC, 12 Union Road, Cambridge, CB2 1EZ, UK, (fax: + 44-1223-33-336033; e-mail: deposit@ccdc.cam.ac.uk or www.ccdc.cam.ac.uk).

Acknowledgement

This work was supported by the CNRS, France.

References

[1] J.F.W. Keana, Chem. Rev. 78 (1978) 37.
[2] M. Tamura, Y. Nakazawa, D. Shiomi, K. Nozawa, Y. Hosokoshi, M. Ishikawa, M. Takahashi, M. Kinoshita, Chem. Phys. Lett. 186 (1991) 401.
[3] R. Chiarelli, M. Novak, A. Rassat, J. Tholence, Nature 363 (1992) 147.
[4] E. Hermandez, M. Mas, E. Molins, C. Rovira, J. Veciana, Angew. Chem., Int. Ed. Engl. 32 (1993) 882.
[5] K. Inoue, H. Iwamura, Chem. Phys. Lett. 207 (1993) 551.
[6] A. Yamaguchi, K. Awaga, T. Inabe, T. Nakamura, M. Matsumoto, Y. Maruyama, Chem. Lett. (1993) 1443.
[7] M. Okumura, K. Yamaguchi, K. Awaga, Chem. Phys. Lett. 228 (1994) 575.
[8] J. Cirujeda, M. Mas, E. Molins, F.L. de Panthou, J. Laugier, J.G. Park, C. Paulsen, P. Rey, P. Rovira, J. Veciana, J. Chem. Soc. Chem. Commun. (1995) 709.
[9] T. Okuno, T. Otsuka, K. Awaga, J. Chem. Soc. Chem. Commun. (1995) 827.
[10] A. Caneschi, F. Ferraro, D. Gatteschi, A. de Lirzin, M.A. Nova, E. Rentschler, R. Sessoli, Adv. Mater. 7 (1995) 476.
[11] J. Veciana, J. Cirujeda, C. Rovira, E. Molins, J. Novoa, J. Phys. 1 France 6 (1996) 1967.
[12] M.M. Matsushita, A.I. Izuoka, T. Sugawara, T. Kobayashi, N. Wada, N. Takeda, M. Ishikawa, J. Am. Chem. Soc. 119 (1997) 4369.
[13] S. Nakatsuji, H. Anzai, J. Mater. Chem. 7 (1997) 2161.
[14] S. Pillet, M. Souhassou, Y. Pontillon, A. Caneschi, D. Gatteschi, C. Lecomte, New. J. Chem. 25 (2001) 131.
[15] A. Bencini, C. Benelli, D. Gatteschi, C. Zanchini, J. Am. Chem. Soc. 106 (1984) 5813.
[16] A. Caneschi, D. Gatteschi, J. Laugier, P. Rey, J. Am. Chem. Soc. 109 (1987) 2191.
[17] A. Caneschi, D. Gatteschi, A. Grand, J. Laugier, P. Rey, L. Pardi, Inorg. Chem. 27 (1988) 1031.
[18] A. Caneschi, D. Gatteschi, R. Sessoli, P. Rey, Acc. Chem. Res. 22 (1989) 392.
[19] A. Caneschi, F. Ferraro, D. Gatteschi, P. Rey, R. Sessoli, Inorg. Chem. 29 (1990) 1756.
[20] A. Caneschi, F. Ferraro, D. Gatteschi, P. Rey, R. Sessoli, Inorg. Chem. 29 (1990) 4217.
[21] A. Caneschi, D. Gatteschi, P. Rey, Prog. Inorg. Chem. 39 (1991) 331.
[22] F. Lanfranc de Panthou, D. Luneau, R. Musin, L. Öhrström, A. Grand, P. Turek, P. Rey, Inorg. Chem. 32 (1993) 3484.
[23] D. Luneau, G. Risoan, P. Rey, A. Grand, A. Caneschi, D. Gatteschi, J. Laugier, Inorg. Chem. 32 (1993) 5616.
[24] G. Ulrich, R. Ziessel, D. Luneau, P. Rey, Tetrahedron Lett. 35 (1994) 1211.
[25] D. Luneau, J. Laugier, P. Rey, G. Ulrich, R. Ziessel, P. Legoll, M. Drillon, J. Chem. Soc., Chem. Commun. (1994) 741.
[26] K. Inoue, T. Hayamizu, H. Iwamura, D. Hashizume, Y. Ohashi, J. Am. Chem. Soc. 118 (1996) 1803.
[27] V. Laget, S. Rouba, P. Rabu, C. Hornick, M. Drillon, J. Magn. Magn. Mater. 154 (1996) 1107.
[28] Z.H. Jiang, B.W. Sun, D.Z. Liao, G.L. Wang, B. Donnadieu, J.P. Tuchagues, Inorg. Chim. Acta 279 (1998) 76.
[29] F.M. Romero, D. Luneau, R. Ziessel, Chem. Commun. (1998) 551.
[30] D. Luneau, F.M. Romero, R. Ziessel, Inorg. Chem. 37 (1998) 5078.
[31] M.L. Kahn, J.P. Sutter, S. Golhen, P. Guinneau, L. Ouahab, O. Kahn, D. Chasseau, J. Am. Chem. Soc. 122 (2000) 3413.
[32] F. Mathevet, D. Luneau, J. Am. Chem. Soc. 123 (2001) 7465.
[33] O. Kahn, Molecular Magnetism, VCH, New York, 1993.
[34] D. Gatteschi, O. Kahn, Molecular Magnetic Materials, HCM Networks, Communauté Européenne, Bruxelles, 1996.
[35] D. Gatteschi, Current Opinion in Solid state and Material Science (1996).
[36] P.L. Lahti, Magnetic Properties of Organic Materials, Dekker INC., New-York- Basel, 1999.
[37] V. Laget, C. Hornick, P. Rabu, M. Drillon, P. Turek, R. Ziessel, Adv. Mater. 10 (1998) 1024.
[38] P. Gerbier, C. Guérin, J. le Bideau, K. Vallé, Chem. Mater. 12 (2000) 264.

[39] A. Togni, L.M. Venanzi, Angew. Chem., Int. Ed. Engl. 33 (1994) 497.
[40] T.V. Laine, M. Klinga, M. Leskelä, Eur. J. Inorg. Chem. (1999) 959.
[41] R.E. Rülke, J.G.P. Delis, A.M. Groot, C.J. Elsevier, P.W.N.H. van Leeuwen, K. Vrieze, K. Goubitz, H. Schenk, J. Organomet. Chem. 508 (1996) 109.
[42] R.L. Huff, S.A. Svejda, D.J. Tempel, M.D. Leatherman, L.K. Johnson, M. Brookhart, Polymer Preprints (Am. Chem. Soc. Div. Polym. Chem.) 42 (2000) 401.
[43] E.F. McCord, S.J. McLain, L.T.J. Nelson, S.D. Arthur, E.B. Coughlin, S.D. Ittel, L.K. Johnson, D. Tempel, C.M. Killian, M. Brookhart, Macromolecules 34 (2001) 362.
[44] A.C. Gottfried, M. Brookhart, Macromolecules 36 (2003) 3085.
[45] R.B. Weisenfeld, J. Org. Chem. 51 (1986) 2434.
[46] C. Morat, A. Rassat, Tetrahedron 28 (1972) 735.
[47] H. Lemaire, Y. Marechal, R. Ramasseule, A. Rassat, Bull. Soc. Chim. (1965) 372.
[48] A.R. Forrester, R.H. Thomson, Nature 203 (1964) 74.
[49] A. Calder, A.R. Forrester, Chem. Commun. (1967) 682.
[50] A. Calder, A.R. Forrester, J. Chem. Soc. C (1969) 1459.
[51] G. Van Koten, K. Vrieze, Adv. Organomet. Chem. 21 (1982) 151.
[52] R. Brière, R.-M. Dupeyre, H. Lemaire, C. Morat, A. Rassat, P. Rey, Bull. Soc. Chim. (1965) 3290.
[53] EPR Brucker simulation program.
[54] B.L. Small, M. Brookhart, A.M.A. Bennett, J. Am. Chem. Soc. 120 (1998) 4049.
[55] B.L. Small, M. Brookhart, Macromolecules 32 (1999) 2120.
[56] G.J.P. Britovsek, V.C. Gibson, B.S. Kimberley, P.J. Maddox, S.J. McTavish, G.A. Solan, A.J.P. White, D.J. Williams, Chem. Commun. (1998) 849.
[57] E.C. Alyea, P.H. Merrel, Syn. React. Inorg. Metal-Org. Chem. 4 (1974) 535.
[58] J.C. Stowell, J. Org. Chem. 36 (1971) 3055.
[59] A.R. Forrester, S.P. Hepburn, J. Chem. Soc. C (1971) 3322.
[60] M. Kitano, N. Koga, H. Iwamura, Inorg. Chem. 33 (1994) 6012.
[61] K. Inoue, H. Iwamura, Angew. Chem., Int. Ed. Engl. 34 (1995) 927.
[62] G.M. Sheldrick, SHELX 86, A Program for Crystal Structure Solution, Institut für Anorganische Chemie de Universität Göttingen, Germany, 1986.
[63] G.M. Sheldrick, SHELX 93 A Program for Crystal Structure Determination, Institut für Anorganische Chemie de Universität Göttingen, Germany, 1993.
[64] W.C. Wolsey, J. Chem. Ed. 50 (1973) A335.
[65] R.V. Cartwright, Chem. Eng. News 61 (1983) 4.
[66] A. Calder, A.R. Forrester, P.G. James, G.R. Luckhurst, J. Am. Chem. Soc. 91 (1969) 3724.